

## **Detection and forecast of the rainy seasons, application over Analamanga ( -18S: -20S and 46E:48E)**

N. Havana Razanatompoharimanga<sup>a</sup>

Doctorate School of Physics and Applications, Dynamic of the Atmosphere, the Climate and the Oceans (DYACO) Laboratory, University of Antananarivo, 101 Antananarivo, Madagascar

**Author(s)' name:** Niry Havana Razanatompoharimanga

**Academic degree and affiliation:** Doctor, Doctorate School of Physics and Applications, <sup>a</sup>Dynamic of the Atmosphere, the Climate and the Oceans (DYACO) Laboratory, University of Antananarivo, 101 Antananarivo, Madagascar

**Corresponding author:** Niry Havana Razanatompoharimanga

**Address:** Dynamic of the Atmosphere, the Climate and the Oceans (DYACO) laboratory, University of Antananarivo, 101 Antananarivo, Madagascar

**e-mail:** [kalahavana@gmail.com](mailto:kalahavana@gmail.com)

**phone number:** +261 34 93 065 57

### **Abstract**

Changes like decrease of the rainfall amount or late rainy seasons are observed over Madagascar nowadays due to the climate changes. To tackle the negative impacts of climate changes, this paper aims to detect rainy seasons period (onset dates and offset dates) in order to forecast rainy season and set calendar. Climate variables, from 1979 to 2021, such as the daily precipitations, the temperatures, the Dipole Index Mode and the Oceanic Niño Indexes) were used. The detection of the rainy seasons was done by the mean of the accumulation of the anomalies of the daily mean of the precipitations. Modelling and forecasting stages were made by using Fuzzy Logic with triangular membership functions. The skill scores were the Root Mean Squared Error (RMSE), the Mean Absolute Error (MAE), the RMSE and MAE scaled by the standard deviation and the average of the onset and demise dates of the rainy seasons. Findings show that the investigated region was subdivided into two regions: A, where the climatological wet spell starts between 25<sup>th</sup> October and 12<sup>th</sup> November, and B, where the climatological wet spell starts between November 16 and 20. The best forecasting models were observed with values of RMSE (MAE) between 0.52 and 0.80 (0.04 and 0.36). Moreover, scaled by the standard deviation (average), these skill scores are less than 1 (have values between 0.05% and 7.30%).

### **Keywords**

Analamanga, Rainy seasons, Onset dates, Cessation dates, Forecasting, Modelling, Fuzzy Logic

## 1. Introduction

Whether in winter [1] or throughout the year, the crop yield relies on the precipitation. However, the climate change influences the wet spell, the rainfall frequencies and the amount of rain-day [2]. Moreover, [3] cited the developing countries as vulnerable to climate change. Not only does climate change has impacts on socio-economic and health [4] but it also generates negative impacts on agriculture and the crop yields [5, 6, 7, 8]. Changes regarding the wet spells and the amount of precipitations were projected over Madagascar [9]. Furthermore, decrease (increase) in annual rainfall are observed over the eastern(southern) part of the island [10, 11].

The knowledge of the onset dates and withdrawal dates of the rainy seasons play a significant role in developing countries where the economy relies on farming and breeding. According to [12] and [13], farming and agricultural sector of Madagascar use more than 70 % of the labor force and represent about 30 % of the Gross Domestic Products of the country. Previous works on precipitations and the rainy seasons over Madagascar were done. [14] and [15] tried to forecast the precipitations regarding the temperatures and the wind speed. [16] concluded that the wind at the 700hPa and 850hPa air pressure levels behave like the precipitation of the austral summers of Madagascar. [17] found that the Indian Ocean Dipole and the El Niño phenomena have links with the rainfall of the Indian Monsoon over the South-East part of Africa. [18] demonstrated that the rainfall over Madagascar is connected to the sea surface temperature of the Indian Ocean. According to [19] and [20], the phenomenon ENSO has an impact on the precipitations of Madagascar. Moreover, the same phenomenon plays a role on the length of the rainy seasons of the Island [21]. However, the climate change has effects on these climatic variables, this leads to the huge variations and changes of the behaviours of the rainy seasons and the precipitations. [22] and [23] exacerbated a significant variability over the Indian Ocean. Furthermore, the climate change plays a role on the delay of the rainy seasons and the persistence of the dry spells over some parts of Madagascar [24]. These situations make the detection of the rainy seasons period difficult. Different forecasting models were developed to better fit these changes. [25] used the Auto-Regressive Integrated Moving Average (ARIMA), [14] and [15] used Fuzzy Logic for forecasting the precipitation, and even [16] and [26] modelled and forecasted the rainy seasons by the mean of Holt-Winters exponential smoothing. To face changes and to tackle the impacts due to these negative effects of climate changes, this work aims to model in order to forecast the rainy seasons and make projection closer to the reality by the mean of Fuzzy Inference System.

## 2. Materials and Methods

Limited by the longitudes 46°E and 48°E and the latitudes -18°S and -16°S (Figure 1), the zone of interest is observed over the central part of Madagascar: Analamanga. Climatic variables, from 1979 to 2021, such as daily precipitations from Climate Hazards Group Infrared Precipitation with Station data (CHIRPS) [27], temperatures from European Centre For Medium Range weather forecast (ECMWF) [28], Oceanic Niño Index and the Dipole Index Mode from National Oceanic and Atmospheric Administration (NOAA) denoted respectively hereinafter ONI [29], DIM, WDIM and EDIM [30] were used with Matlab.

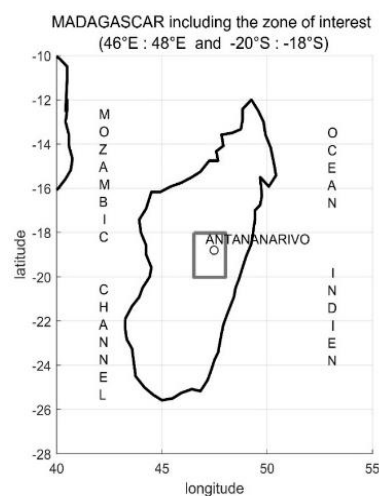


Figure 1: The zone of interest

Different definitions of the onset and the withdrawal dates of the rainy season [31, 32, 33] were used to detect wet spell throughout a year. In this paper, the onset and the cessation dates of the rainy seasons from 1981 to 2021 and the climatological wet period over all grid points were identified by applying the definitions of [34, 35, 36]. The zone of interest was divided into two regions: A and B regarding its climatological onset dates. Four serial data corresponding, each, to the spatial average: data corresponding to the onset and cessation dates over A and B denoted hereinafter OA, OB, CA and CB respectively were created. The correlation between OA, OB, CA and CB and the climatological variables such as the temperatures, the DIM and the ONI was analysed by the mean of the Pearson's correlation coefficient in order to define some predictors of the rainy seasons. 95% significant correlation coefficients were kept. Different predictors were defined regarding their own Pearson's correlation coefficients (Table 1). The value between brackets with a negative sign represents

the number of years which precedes the actual rainy season. So, 0 represents the same year as the year of the rainy season.

Table 1: Pearson's correlation coefficients 'r' corresponding to the different predictors

Predictors	OA		OB	
	month (year)	r	month (year)	r
<b>ONI</b>	April (-2)	0.34	May (-2)	0.36
	May (-2)	0.36	June (-2)	0.31
<b>DIM</b>	February (-3)	0.31	February (-3)	0.38
			July (-3)	0.38
<b>WDIM</b>				
<b>EDIM</b>	January (-3)	0.38		
	February (-3)	0.38		
	March (-3)	0.38		
<b>Temperatures in September</b>	Minimal temperature (0)	-0.33	Maximal Temperature (0)	-0.34
	Average Temperature (0)	-0.32		
	CA		CB	
<b>DIM</b>	February (-3)	0.31	January (-5)	0.32
			February (-4)	0.32
<b>EDIM</b>			February (-3)	0.38
	May (-5)	0.38	January (-5)	0.32
	January (-3)	0.38	July (-3)	0.38
<b>WDIM</b>	February (-3)	0.38		
	March (-3)	0.38	May (-5)	0.33
			December (-5)	0.36

The model, the validation and the forecast of the onset and cessation dates were realised by the mean of Fuzzy Logic (FL). Some definitions and explanation regarding Fuzzy Logic were described by [37]. On one hand, [15, 14, 38] defined linguistic variables for forecasting the precipitations through other climatic variables. On the other hand, [39,40] applied the definition of the agronomic onset date over West Africa on the Fuzzy membership function in order to detect and forecast the onset dates of the agronomic wet spells. In this work, none clustering to create linguistic variables was done. Each observation of the variable possesses its own equation (Equation 1) related to a triangular membership function (Figure 2).

$$\mu(x_a) = \begin{cases} 0 & \text{if } x_a \leq m - k \text{ et } x_a \geq m + k \\ \frac{x_a - (m - k)}{m - (m - k)} & \text{if } m - k \leq x_a \leq m \\ \frac{(m + k) - x_a}{(m + k) - m} & \text{if } m \leq x_a \leq m + k \end{cases} \quad (1)$$

where ' $x_a$ ' is the observed data in year 'a'; 'm' is the value of the observation, 2k is the base of the triangle (Figure 2), and  $\mu(x_a)$  is the membership degree corresponding to the variables.

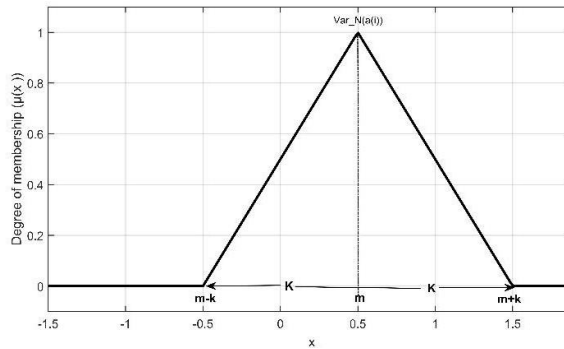


Figure 2: A representation of a triangular membership function

As can be seen in Figure 2, the maximum membership degree is reached with the value of the observed variable denoted 'm'.

33(31) equations corresponding to the 33(31) years related to the training were developed. 33 and 31 samples of triangular membership functions corresponding to some climatic variables were represented graphically in Figure 3. As a result, 33 and 31 rules were created according to the rule base if ... and ... then (Equation 2):

$$\text{if } (\text{var1}(a_i)) \text{ and } (\text{var2}(a_i)) \text{ and } (\text{var3}(a_i)) \text{ and } \dots (\text{varN}(a_i)) \text{ then } (\text{Var\_output}(a_i)) \quad (2)$$

$a_i$  is the year at rank i which ranges from 1 to 33 or 31.

var1, var2, ..., varN are the predictors and Var\_output correspond to OA, OB, CA and CB.

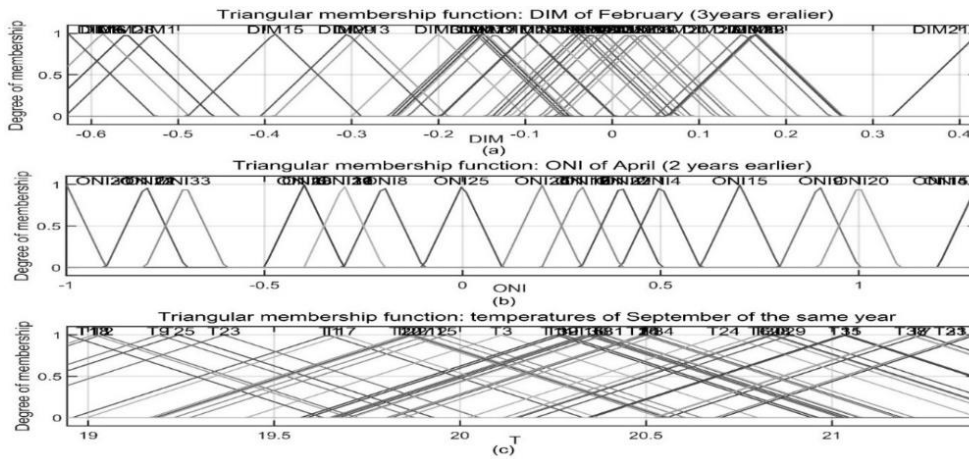


Figure 3: Examples of triangular membership functions related to: Dipole Index Mode (a) ;  
Oceanic Niño Index (b) and temperatures (c)

Different ranges of the parameter 'k' were used according to the input and output variables, Table 2, in order to find the best forecasting models. The maximum value of 'k' refers to the standard deviation of the serial data of the predictors. Regarding the outputs: OA, OB, CA and CB, the value of the parameter 'k' is one week.

Table 2: Different ranges of the parameter 'k' related to the predictors and the outputs

k	Predictors	Output
0.01 to 0.3 with a step equal to 0.05 (0.01:0.05:0.3)	ONI	OA and OB
0.01 to 0.1 with a step equal to 0.01 (0.01:0.01:0.1)	DIM	OA and OB
0.1 to 0.8 with a step equal to 0.1 (0.1:0.1:0.8)	Temperatures	OA and OB
0.01 to 0.3 with a step equal to 0.02 (0.01:0.02:0.3)	DIM	CA and CB

The best training models were chosen with the values of 'k' which correspond to the minima values of the Root Mean Squared Error (RMSE). Different values of the RMSE related to the different values of the parameter 'k' are shown in Figure 4. The solid(dashed) lines depicts the RMSE related to the validation(model) regarding different values of 'k'.

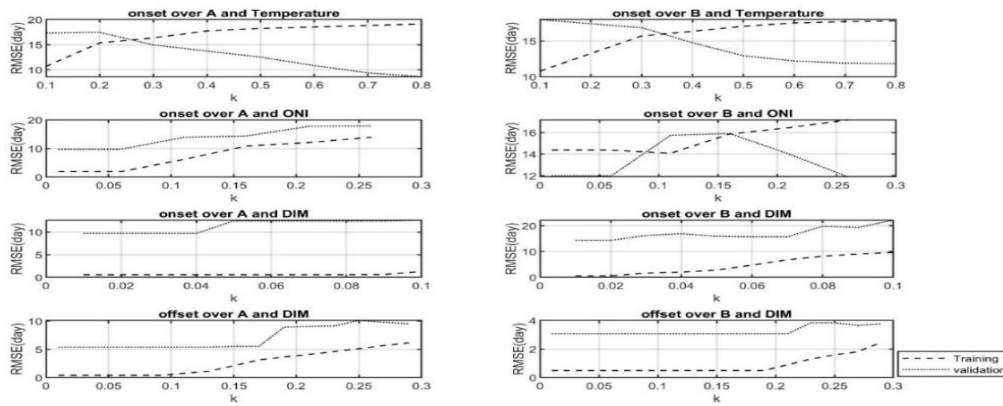


Figure 4: Different values of RMSE related to different values of 'k' corresponding to the training (---) and the validation (...) of the onset and cessation dates of the rainy seasons over A and B

80% of the serial data were kept for training and 20% were set aside for the validation and testing the model. Consequently, over 41 years (1981-2021) and over 38 years (1981-2018), 33 years and 31 years were kept for training respectively.

Different skill scores: RMSE, Mean Absolute Error (MAE), RMSE and MAEE scaled by the standard deviation denoted hereinafter rRMSE and rMAE, RMSE and MAE scaled by the average denoted hereinafter nRMSE and nMAE were used in order to verify the accuracy of the forecasting models. rRMSE and rMAE can show if the error is less than the climatological standard deviation. nRMSE and nMAE measure, in percent, the relative amount between the error and the climatological average. The less value of nRMSE and nMAE we observe, according to [41], with a certain percentage, the better the forecasted data are.

### 3. Results

The fluctuation of the onset and cessation dates of the rainy seasons from 1981 to 2021 over the regions A and B are shown in Figure 5.

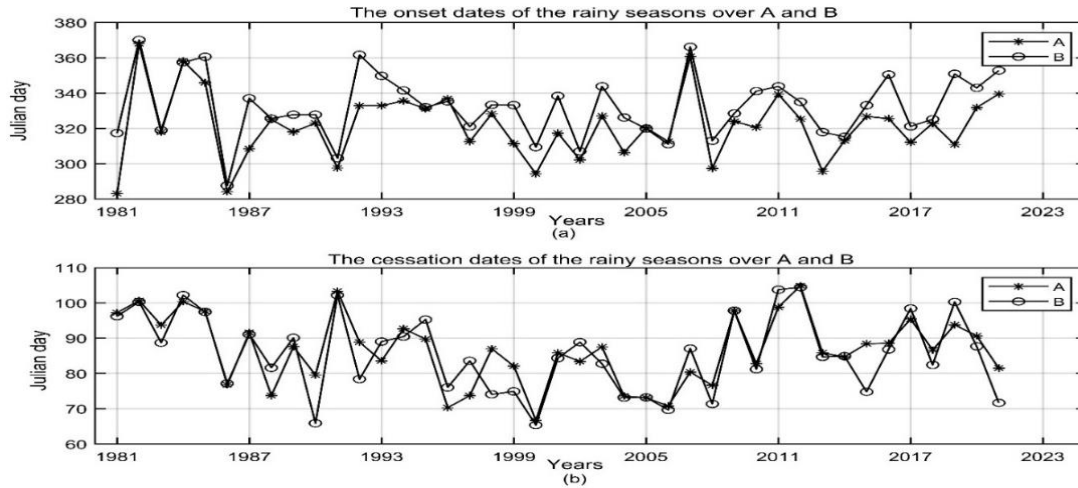


Figure 5: Evolution of the onset (a) and cessation (b) dates of the rainy seasons over both regions A and B from 1981 to 2021)

Figure 5 depicts the onset-dates of rainy seasons, over the region A and the region B, which fluctuate between the 280th day and 15<sup>th</sup> days of the next year. Over A(B), the minimum was registered in 1981(1986). The maximum was observed in 1982 for both regions. The cessation dates of the rainy seasons fluctuate between the 63<sup>th</sup> and 106<sup>th</sup> day of the calendar year from 1981 to 2021 over both regions. The minimum (maximum) was registered in 2000(2012) over the region A. The minimum (maximum) was detected in 2000(2011) over the region B. The climatological onset and cessation dates of the rainy seasons over all the grid points within the zone of interest were presented in Figure 6 and Figure 7 respectively in the form of a map.

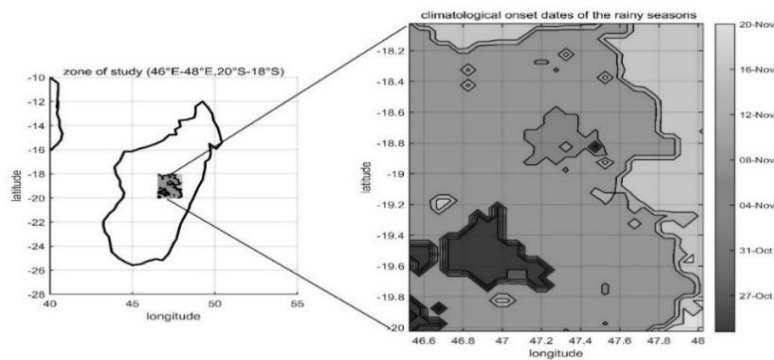


Figure 6: Spatial distribution of the climatological onset dates of the rainy seasons from 1981 to 2021 over the zone of interest

As can be seen in Figure 6, significant part of the zone of interest possesses climatological rainy seasons which starts between 25<sup>th</sup> October and 15<sup>th</sup> November, denoted region A. The Eastern and the Northern part possess climatological rainy seasons which start between 16<sup>th</sup> and 20<sup>th</sup> November, denoted region B.

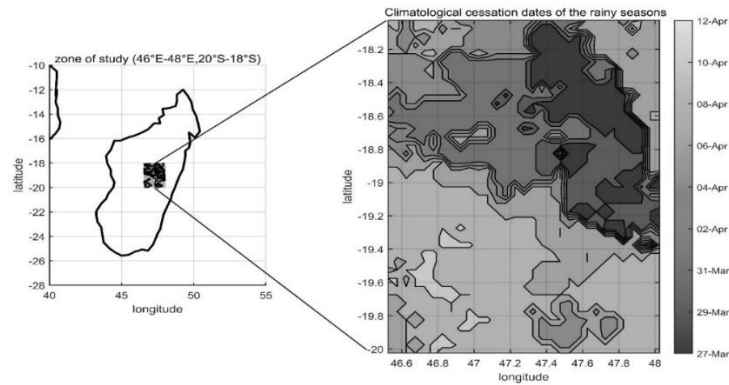


Figure 7: Spatial distribution of the climatological cessation dates of the rainy seasons from 1981 to 2021 over the zone of interest

Figure 7 shows the spatial variation of the climatological cessation dates over all the grid points. The North-Eastern, the Southern and the South-Western parts possess climatological rainy seasons which end between 8<sup>th</sup> and 12<sup>th</sup> April. The Eastern and North-Eastern part possess climatological rainy seasons which end between 27<sup>th</sup> March and 4<sup>th</sup> April. Modelling and forecasting of the onset and cessation dates of the rainy seasons over both regions are shown in Figure 8, Figure 9 and Figure 10.

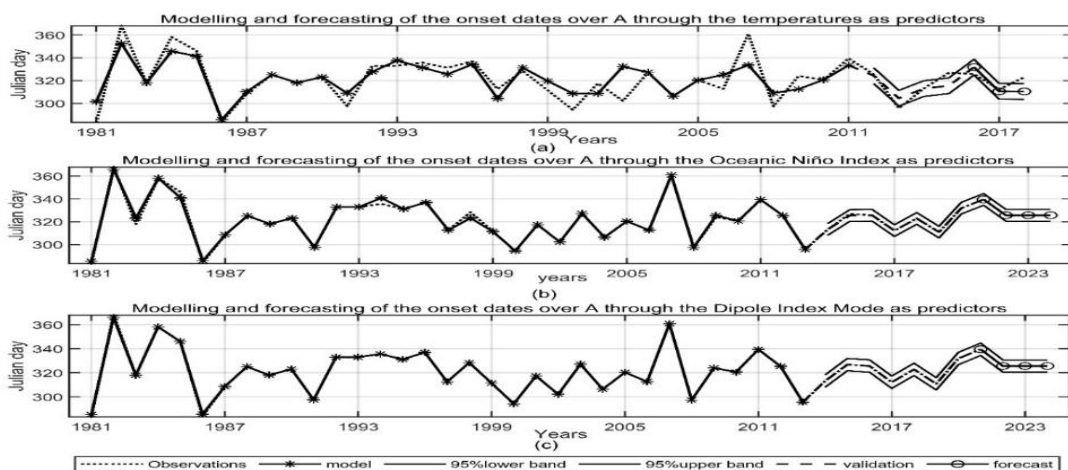


Figure 8: Modelling and forecasting of the onset dates of the rainy seasons with three predictors: the temperatures (a); the Oceanic Niño Index (b) and the Dipole Mode Index (c) over A

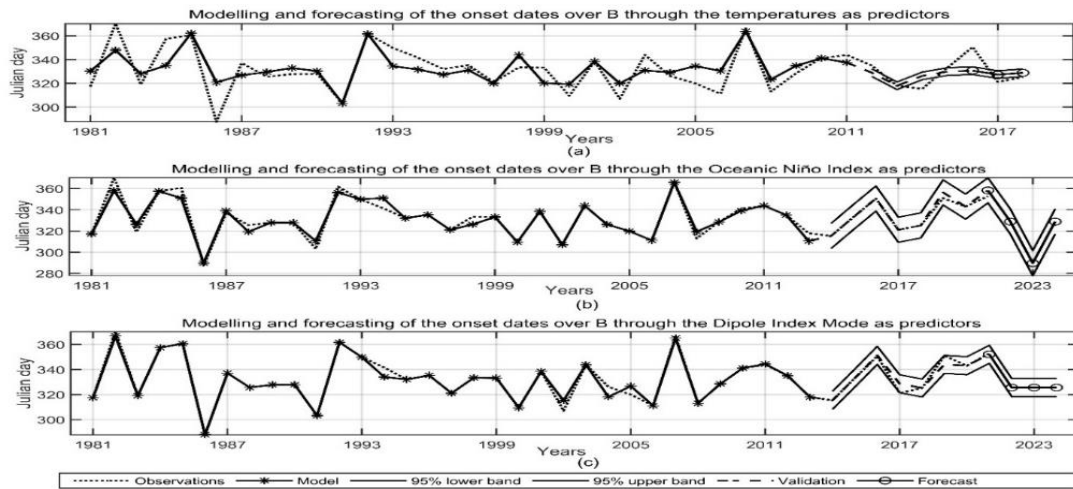


Figure 9: Modelling and forecasting of the onset dates of the rainy seasons with three predictors: the temperatures (a); the Oceanic Niño Index (b) and the Dipole Mode Index (c) over B.

Figure 8 and Figure 9 show that, with temperatures as predictors(a), the-curves of the predicted variables do not overlap very well the curve of the actual data. However, with ONI (b) and DIM (c) as predictors, the curves of the predicted variables overlap the curves of the observed variables. Regarding the cessation dates, Figure 10 the forecasted dates overlap the observed dates.

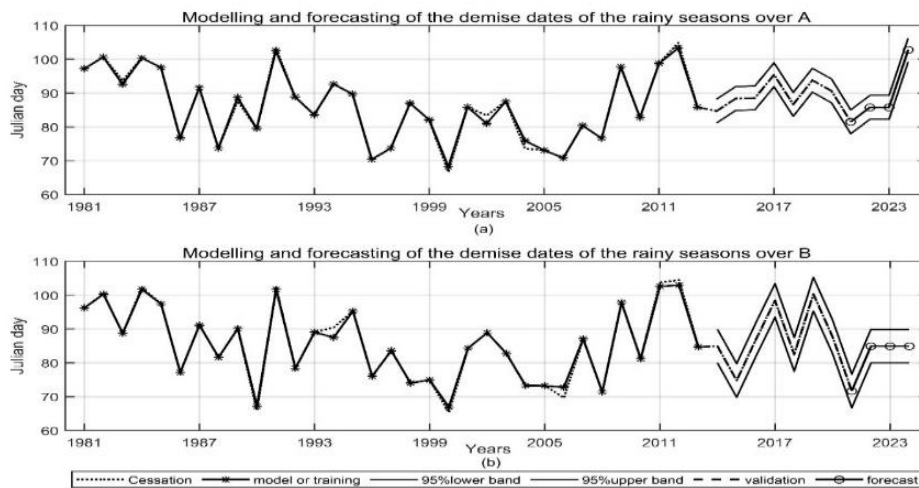


Figure 10: Modelling and forecasting of the cessation dates of the rainy seasons with the predictors: the Dipole Mode Index over A (a) and B (b)

Different skill scores values of the forecasting models of the onset and cessation dates related to the different predictors are given in Table 3.

Table 3: Different values of RMSE, rRMSE, nRMSE, MAE, rMAE and nMAE as forecast accuracy measure (skill score)

<i>Onset over A</i>				<i>Onset over B</i>		
<i>predictors</i>	RMSE	rRMSE	nRMSE(%)	RMSE	rRMSE	nRMSE(%)
<i>T</i>	13.78	0.73	4.29	8.14	0.45	2.45
<i>ONI</i>	1.73	0.09	0.54	4.18	0.23	1.26
<i>DIM</i>	0.52	0.03	0.16	0.57	0.03	0.17
Cessation over A				cessation over B		
<i>DIM</i>	0.76	0.08	0.87	0.80	0.07	0.94
Onset over A				Onset over B		
	MAE	rMAE	nMAE	MAE	rMAE	nMAE
<i>T</i>	13.74	0.73	7.30	2.20	0.40	4.27
<i>ONI</i>	0.72	0.04	2.33	0.70	0.13	0.22
<i>DIM</i>	0.14	0.01	0.12	0.04	0.01	0.05
Cessation over A				cessation over B		
<i>DIM</i>	0.33	0.03	0.31	0.36	0.03	0.39

The forecasting model of OA(OB) linked to the temperatures, *Table 3*, possesses a value of RMSE being 13.78 days (8.14 days) and a value of MAE being 13.74 days (2.20 days). The minima values of RMSE and MAE correspond to the forecasting models linked to DIM over both regions. Furthermore, the values of rRMSE and rMAE are less than 1. The calendar of the rainy seasons is set in *Table 4*.

Table 4: Forecast of the onset dates and the demise dates of the rainy seasons over the region A and the region B, with each, their error in days

	<i>region A</i>	<i>region B</i>
<i>Predictors</i>	Onset dates	
<i>Temperatures</i>	06/11/2017(±7)	23/11/2017(±3)
	06/11/2018(±7)	25/11/2018(±3)
<i>ONI</i>	22/11/2022(±5)	25/11/2022(±12)
	22/11/2023(±5)	17/10/2023(±12)
	23/11/2024(±5)	26/11/2024(±12)
<i>DIM</i>	22/11/2022(±5)	22/11/2022(±7)

	22/11/2023(±5)	22/11/2023(±7)
	23/11/2024(±5)	23/11/2024(±7)
	Demise dates	
<i>DIM</i>	27/03/2022(±4)	26/03/2022(±5)
	27/03/2023(±4)	26/03/2023(±5)
	14/04/2024(±4)	27/03/2024(±5)

With ONI and DIM as predictors, the rainy seasons over A(B) is supposed to start on 22<sup>nd</sup> (25<sup>th</sup>) November in 2022 and 2023 (17<sup>th</sup> October 2023) and on 23<sup>rd</sup> (26<sup>th</sup>) November 2024. and supposed to end on 27<sup>th</sup>(26<sup>th</sup>) March in 2022 and 2023 and on 14<sup>th</sup> April (27<sup>th</sup> March) 2024.

#### 4. Discussion

From Figure 5, earlier onset over A(B) was observed on 9<sup>th</sup>(5<sup>th</sup>) October 1981 and in 1982, the rainy season started later than normal start: on 5<sup>th</sup>(7<sup>th</sup>) January over A(B). Earlier demise dates of rainy seasons were registered on 5<sup>th</sup>(6<sup>th</sup>) March 2000 over A(B). Late demise date was observed on 14<sup>th</sup> April 2012 over A. The Eastern and North part of the zone of interest, region B, Figure 6, possesses a late climatological rainy season than the region A. A Southwest-Northeast gradient is observed, Figure 6, regarding the onset dates of the climatological rainy seasons. The climatological cessation dates over all grid points within the zone of interest, Figure 7, barely vary with a discrepancy of two days.

All forecasting models have small values of RMSE and MAE (Table 3). Furthermore, with a value of nRMSE  $\leq 15\%$  [41], all the models are defined 'good'. The forecasting models of the rainy seasons related to the DIM as predictors are the best models. That would be related to the geographical situation of the Indian Ocean Dipole. The forecast of onset date of the rainy season in 2023 is quite earlier than the others, 17<sup>th</sup> October (Table 4), this forecast is related to the ONI in May and June of the year 2021 (Table 1). A late forecast of the demise date, 14<sup>th</sup> April 2024 (Table 4) over A is linked to the January DIM of 2021, the May EDIM [30] in 2019, the January, February and March EDIM [30] of the year 2021 (Table 1). As can be seen in Table 4, the best forecasting models possess an error varying between 4 days and one week.

The training models of the onset dates related to the temperatures (Figure 4) over both regions lose its accuracies when the value of 'k' increases. However, the more the value of 'k' increases, the better the quality of the validation of the model. This means, the smaller (larger) the base of the triangular membership function is, the better the training models (validations of the model) are. This might be another issue for improving the rainy seasons forecasting model related to the temperatures.

## 5. Conclusion

To tackle the negative impacts of climate changes, this work aims to model and forecast the rainy seasons of Analamanga accurately by the mean of Fuzzy Logic.

The detection of the onset and cessation dates of the rainy seasons led to the subdivision of the zone of interest into two regions. Denoted region A, it possesses climatological rainy periods which start between 25<sup>th</sup> October and 15<sup>th</sup> November. Denoted region B, it possesses climatological rainy seasons which start from 16<sup>th</sup> November.

The use of the Pearson's coefficient correlations led to the determination of some predictors, such as the ONI, the DIM, the EDIM, the WDIM [30] and the temperatures, of the onset and cessation dates of the rainy seasons over both regions A and B.

The Fuzzy Inference System with its triangular membership function was used to model and forecast the rainy seasons. Values of RMSE and MAE being less than 14 days were observed. Moreover, values of nRMSE and nMAE were less than 10%. This leads us to conclude that the models are 'good' [41]. Values of rRMSE and rMAE less than 1 lead us to conclude that the forecasting model of the rainy seasons over Analamanga by the mean of the FL with the triangular membership functions are excellent. Actually, the output of the models possesses errors less than the standard deviation of the serial data of the observed onset and cessation dates. After comparing the forecasting models related to the different predictors, the best one is the forecasting models of the rainy seasons related to the DIM over both regions.

Nevertheless, the choice of the base, related to the parameter 'k', of the triangular membership functions plays an important role in the choice of the best model throughout the training and the validation. An analyse in depth of the choice of the parameter 'k' should be a focus in future proposal for improving the forecasting model of the rainy seasons. Moreover, other climatic variables with a high values of Pearson's coefficient correlation might be used as predictors of the rainy seasons. An investigation of the same method on Sub-seasonal to Seasonal(S2S) data can be of interest to future researches.

## 6. **Aknowledgements**

I am thakfull to Professor Amadou T. Gaye, Dr. Dahirou Wane and Dr. Abdou Lahat Dieng from the University Cheikh Anta Diop of Dakar (UCAD), for helping me retrieving the precipitations data.

## 7. References

- [1] Tulkin, F., S. Umarov, T. Hilorme, B. Khasanov, and A. Durmanov, “The Impact of Energy Aspects on the Climatic Indicators of Agricultural Products”, *International Journal of Energy, Environment, and Economics*, Vol. 30, no. 2, pp.187-209, 2022.
- [2] 2 Lawal, A. and A. M. Yamusa, “Changing Pattern of Rainfall Amount and Raindays in Samaru, Northern Nigeria and Their Implications on Crop Production”, *World Journal of Agricultural Research*, vol. 8, no. 4, pp.134-141, 2020, doi: 10.12691/wjar-8-4-5.
- [3] Christensen, J.H., B. Hewitson, A. Busuioc, A. Chen, X. Gao, I. Held, R. Jones, R.K. Kolli, W.-T. Kwon, R. Laprise, V. Magaña Rueda, L. Mearns, C.G. Menéndez, J. Räisänen, A. Rinke, A. Sarr, and P. Whetton, “Regional Climate Projections. In: Climate Change 2007: The Physical Science Basis”, Contribution of Working Group I to the Fourth Assessment Report of the Intergovernmental Panel on Climate Change, 2007, *Cambridge University Press Cambridge*, United Kingdom and New York, NY, USA.
- [4] A. Z. Shaheen, “Perception of Pakistani Women about Socio-Economic Impact of Climate Change”, *International Journal of Energy, Environment, and Economics*, vol. 29, no. 3, pp. 231-254, 2021.
- [5] Habib-ur-Rahman, M., Ahmad, A., Raza, A., Hasnain, M. U., Alharby, H.F., Alzahrani, Y. M., Bamagoos, A. A., Hakeem, K. R., Ahmad, S., Nasim, W., Ali, S., Mansour, F. and E. L. Sabagh, A., “Impact of climate change on agricultural production; Issues, challenges, and opportunities in Asia”, *Front. Plant Sci.*, 13:925548, 2022, doi: 10.3389/fpls.2022.925548  
<https://www.frontiersin.org/articles/10.3389/fpls.2022.925548/full>.
- [6] Jahan, N., and Salahuddin, M. “The impacts of climate change on agriculture: Evidence from a developing country”, *International Journal of Energy, Environment, and Economics*, vol. 25, no. 3, pp. 175-192, 2017.
- [7] Kuddus, A., Yasmin, F., and Mamun, A. A., “Climate change and agricultural production in Bangladesh: A cointegration and error correction approach”, *International Journal of Energy, Environment, and Economics*, vol. 27, no. 2, pp. 135-149, 2019.
- [8] L. E. Emediegwu, A. Wossink, and A. Hall, “The impacts of climate change on agriculture in sub-Saharan Africa: A spatial panel data approach”, *World*

- Development*, vol. 158, 2022, 105967, ISSN 0305-750X,  
<https://doi.org/10.1016/j.worlddev.2022.105967>.
- [9] R. Barimalala, N. Raholijao, W. Pokam and C. J. C. Reason, “Potential impacts of 1.5 °C, 2 °C global warming levels on temperature and rainfall over Madagascar”, *Environmental Research Letters*, vol. 16, no. 4, 1604019, 2021, doi 10.1088/1748-9326/abeb34.
- [10] L. A. Vincent, E. Aguilar, M. Saidou, A. F. Hassane, G. Jumaux, D. Roy, P. Booneedy, R. Virasami, L. Y. A. Randriamarolaza, F. R. faniriantsoa, V. Amelie, H. Seeward, and B. Montfraix, “Observed trends in indices of daily and extreme temperature and precipitation for the countries of the western Indian Ocean, 1961–2008”, *Journal of Geophysical Research : Atmospheres*, 2011, <https://doi.org/10.1029/2010JD015303>, Online ISSN:2169-8996
- [11] Tadross, M., Randriamarolaza, L., Rabefitia, Z. and Zheng, K. Y., ‘Climate Change in Madagascar: Recent past and Future’, Washington, DC: World Bank, pp. 1-18, 2008.
- [12] Ministère de l’Agriculture et de la Souveraineté Alimentaire, “Madagascar”, 2016, [agriculture.gouv.fr/Madagascar](http://agriculture.gouv.fr/Madagascar)
- [13] Garruchet, V., Bosc, P. M., Mialet-Serra, I., “L’Agriculture à Madagascar : évolution, chiffres clés et défis”, *Saint-Denis : PRéRAD-OI*, pp. 1-88, 2023, <https://www.prerad-oi.org/actualites/2023/44-observatoire-madagascar-faisabilite>.
- [14] Agboola, A.H., Gabriel, A. J., Aliyu, E.O., and Alese, B.K., “Development of a Fuzzy Logic Based Rainfall Prediction Model”, *International Journal of Engineering and Technology*, vol. 3, no. 4, pp. 427-435, 2013.
- [15] Rahman, M., “Improvement of Rainfall Prediction Model by Using Fuzzy Logic”, *American Journal of Climate Change*, Vol. 9, pp. 391-399, 2020, doi: 10.4236/ajcc.2020.94024.
- [16] Nirry Havana Razanatompocharimanga, “Prévision des périodes de pluies (début et fin) dans la partie centre-ouest de Madagascar”, PhD. Thesis, 2016, [http://biblio.univ-antananarivo.mg/pdfs/razanatompocharimanganiryh\\_PH\\_DNR\\_16.pdf](http://biblio.univ-antananarivo.mg/pdfs/razanatompocharimanganiryh_PH_DNR_16.pdf) .
- [17] Wenju, C., G. Wang, Z. Li, X. Zheng, K. Yang, and Benjamin, Ng, “Chapter 21- Response of the positive Indian Ocean dipole to climate change and impact on Indian summer monsoon rainfall”, *Indian Summer Monsoon Variability*, Elsevier, pp. 413-432, 2021, <https://doi.org/10.1016/B978-0-12-822402-1.00010-7>.

- [18] Herijaona, Hani-Roge, Hundilida, Randriatsara, Zhenghua, H., Ayugi, B., Exavery, K. M., Floribert, and V., A. Nkuzimana, “Interannual characteristics of rainfall over Madagascar and its relationship with the Indian Ocean sea surface temperature variation”, *Theoretical and Applied Climatology*, vol. 148, pp. 349-362, 2022.
- [19] Ocha, A., and Simmonds, I. H., “Internannual variability of Southern African summer rainfall. Part II: Modelling the impact of sea surface temperatures on rainfall and circulation”, *Int. J. Clim.*, vol.17, pp. 267-290, 1997.
- [20] Salim A. Ali, Rabeharisoa J. M., A.A. Ratiarison, and Rakotovao, N., ‘El Niño climate disturbance in northern Madagascar and the Comoros’, in: Proc. Intl. Conf. on High-Energy Physics 16, pp. 1-7, 2016, pp.1-6, 2016, [https://www.slac.stanford.edu/econf/C161013/hepmad16\\_talks/salim.pdf](https://www.slac.stanford.edu/econf/C161013/hepmad16_talks/salim.pdf).
- [21] N. Rakotovao, N. Havana, Razanatompoaharimanga, A. A. Ratiarison, and J. Andriaparany, H., “Influence of ENSO and MJO climatic phenomena on rainfall over the west coast of Madagascar”, in: Proc. Intl. Conf. on High-Energy Physics 16, pp. 1-7, 2016, [https://www.slac.stanford.edu/econf/C161013/hepmad16\\_talks/rakotovao.pdf](https://www.slac.stanford.edu/econf/C161013/hepmad16_talks/rakotovao.pdf)
- [22] Brown University, “How climate change impacts the Indian Ocean dipole, leading to severe droughts and floods”, *Science Daily*, 2023, [www.sciencedaily.com/releases/2023/01/230104231744.htm](http://www.sciencedaily.com/releases/2023/01/230104231744.htm)
- [23] Sandeep, Mohapatra, “The Indian Ocean is becoming more active and has started impacting the global climate”, breakthrough in Neliti on climate change, 2022, <https://breakthrough.neliti.com/indian-ocean-climate-change/>.
- [24] Cycloneoi, “les conditions anormalement sèche vont perdurer”, Cycloneoi, Infos climat, 2022, <https://www.cycloneoi.com/archives-blog/infos-diverses/persistence-d-une-anomalie-seche-marquee-sur-le-sud-ouest-ocean-indien.html>.
- [25] N. RAKOTOVAO, ‘Influence de la variabilité intra-saisonnière de la convection dans le canal de Mozambique, de phénomènes Enso et MJO sur la pluviométrie de la côte Ouest de Madagascar’. PhD. Thesis, 2014, [http://biblio.univ-antananarivo.mg/pdfs/rakotovaoNiryA\\_PH\\_DNR\\_14.pdf](http://biblio.univ-antananarivo.mg/pdfs/rakotovaoNiryA_PH_DNR_14.pdf).
- [26] N. Havana, Razanatompoaharimanga, and A. A. Ratiarison, “Study and forecast of rainy seasons at Miarinarivo (19°S, 47°E)”, in: Proc. Intl. Conf. on High-Energy Physics 18, pp. 1-8, 2018, [https://www.slac.stanford.edu/econf/C180906/hepmad18\\_talks/Razanatomp1.pdf](https://www.slac.stanford.edu/econf/C180906/hepmad18_talks/Razanatomp1.pdf).

- [27] Funk, C., Peterson, P., Landsfeld, M., Pedreros, D., J. Verdin, Shraddhanand, S., G. Husak, J. Rowland, L. Harrison, Hoell, A., and Michaelsen, J., “The climate hazards infrared precipitation with stations stations—A new environmental record for monitoring extremes”, *Scientific Data*, vol. 2, no 150066, 2015, [doi.org/10.1038/sdata.2015.66](https://doi.org/10.1038/sdata.2015.66).
- [28] D. P. Dee, S. M. Uppala, A. J. Simmons, P. Berrisford, P. Poli, S. Kobayashi, U. Andrae, M. A. Balmaseda, G. Balsamo, P. Bauer, P. Bechtold, A. C. M. Belijaars, L. Van de Berg, J. Bidlot, N. Bormann, C. Delsol, R. Dragani, M. Fuentes, A. J. Geer, L. Haimberger, S. B. Healy, H. Hersbach, E. V. Hólm, L. Isaksen, P. Kallberg, M. Köhler, M. Matricardi, A. P. McNally, B. M. Monge-Sanz, J. J. Morcrette, B. K. Park, C. Peubey, P. de Rosnay, C. Tavolato, J. N. Thépaut, and F. Vitart, “The ERA-Interim reanalysis: Configuration and performance of the data assimilation system, Q. J. R”, *Meteorol. Soc.*, vol.137, no 656, pp. 553 –597, 2011, <https://doi.org/10.1002/qj.828>.
- [29] NOAA/National Weather Service, “Cold and Warm Episodes by Season”, *Climate Prediction Center*, retrieved from: [https://origin.cpc.ncep.noaa.gov/products/analysis\\_monitoring/ensostuff/ONI\\_v5.hph](https://origin.cpc.ncep.noaa.gov/products/analysis_monitoring/ensostuff/ONI_v5.hph).
- [30] Cathy Smith, “Dipole Mode Index”, Working Groupe on Surface Pressure, NOAA ESRL Physical Sciences Laboratory, 2022, retrieved from [http://psl.noaa.gov/gcos\\_wgps/Timeseries/DMI/index.html](http://psl.noaa.gov/gcos_wgps/Timeseries/DMI/index.html).
- [31] M. V. K. SIVAKUMAR, “Predicting rainy season potential from the onset of rains in southern Sahelian and Sudanian climatic zones of west Africa”, *Agricultural and Forest Meteorology*, vol. 42, pp. 295-305, 1988.
- [32] MARTEAU, R., MORON, V. and PHILIPPON, N., “Spatial coherence of monsoon onset over Western and Central Sahel (1950-2000)”, *Journal of Climate*, vol. 22, no. 5, pp. 1313-1324., 2009.
- [33] A. Khan, Md. G. I. Emran, M. H. Momin, M. Saha, K. T. Ahmed, S. Mahmud, A. K. Das, S. Banerjee, and Syed, H. R., “Study on the Arrival and Withdrawal of Rainy Season in the Central Region of Bangladesh”, *International Journal of Energy, Environment, and Economics*, vol. 30, no.1, pp.1-13, 2022.
- [34] Liebmann, B., I. Bladé, G. N. Kiladis, L. M. Carvalho, G. B. Senay, D. Allured, S. Leroux, and C. Funk, “Seasonality of African Precipitation from 1996 to 2009”, *Journal of Climate*, vol. 25, pp. 4304-4322, 2012.

- [35] Liebmann, B., Camargo, S., Seth, A., J. Marengo, L. M. Carvalho, D. Allured, Fu, R., and C. Vera, “Onset and End of the Rainy Season in South America in Observations and the ECHAM 4.5 Atmospheric General Circulation Model”, *Journal of Climate*, vol. 20, pp. 2037-2050, 2007.
- [36] Wainwright, C., Black, E. and Allan, R., “The onset and cessation of seasonal rainfall over Africa”, *Journal of Geophysical Research: Atmospheres*, vol. 121, no 11, pp.405–11,424, 2016, <https://doi.org/10.1002/2016JD025428>.
- [37] Moraga. Claudio, “Introduction to Fuzzy Logic”, *Facta universitatis - series: Electronics and Energetics*, vol. 18, pp. 319-328, 2005.
- [38] Somia, A. Asklany, K. Elhelow, I.K. Youssef, and M. Abd El-wahab, “ Rainfall events prediction using rule-based fuzzy inference system”, *Atmospheric Research*, vol. 101, pp.228–236, 2011.
- [39] P. Laux, H. Kunstmann, and A. Bardossy, “Predicting the regional onset of the rainy season in west Africa”, *International Journal of Climatology*, vol. 28, no 3, pp.329-342, 2007.
- [40] M. Rauch, J.Bliefernicht, P. laux, S. Salack, M. Waongo and H. Kunstmann, “Seasonal forecasting of the onset of rainy season in West Africa”, *Atmosphere*, vol. 10, no 9, 528, pp. 1-21, 2019, <https://doi.org/10.3390/atmos10090528>
- [41] S. Liu, J.Y. Yang, X.Y. Zhang, C.F. Drury, W.D. Reynolds, and G. Hoogenboom, “Modelling crop yield, soil water content and soil temperature for a soybean -maize rotation under conventional and conservation tillage systems in Northeast China”, *Agricultural Water Management*, vol. 123, pp. 32-44, 2013, [doi.org/10.1016/j.agwat.2013.03.001](https://doi.org/10.1016/j.agwat.2013.03.001).

## 8. Tables

Table 1: Pearson's correlation coefficients 'r' corresponding to the different predictors

Predictors	OA		OB	
	month (year)	r	month (year)	r
<b>ONI</b>	April (-2)	0.34	May (-2)	0.36
	May (-2)	0.36	June (-2)	0.31
<b>DIM</b> <b>WDIM</b> <b>EDIM</b>	February (-3)	0.31	February (-3)	0.38
			July (-3)	0.38
	January (-3)	0.38		
	February (-3)	0.38		
<b>Temperatures in September</b>	Minimal temperature (0)	-0.33	Maximal Temperature (0)	-0.34
	Average Temperature (0)	-0.32		
	CA		CB	
<b>DIM</b>	February (-3)	0.31	January (-5)	0.32
			February (-4)	0.32
<b>EDIM</b>	May (-5)	0.38	February (-3)	0.38
	January (-3)	0.38	January (-5)	0.32
	February (-3)	0.38	July (-3)	0.38
<b>WDIM</b>	March (-3)	0.38	May (-5)	0.33
			December (-5)	0.36

Table 2: Different ranges of the parameter 'k' related to the predictors and the outputs

k	Predictors	Output
0.01 to 0.3 with a step equal to 0.05 (0.01:0.05:0.3)	ONI	OA et OB
0.01 to 0.1 with a step equal to 0.01 (0.01:0.01:0.1)	DIM	OA et OB
0.1 to 0.8 with a step equal to 0.1 (0.1:0.1:0.8)	Temperatures	OA et OB
0.01 to 0.3 with a step equal to 0.02 (0.01:0.02:0.3)	DIM	CA et CB

Table 3: Different values of RMSE, rRMSE, nRMSE, MAE, rMAE and nMAE as forecast accuracy measure (skill score)

<i>Onset over A</i>				<i>Onset over B</i>		
<i>predictors</i>	RMSE	rRMSE	nRMSE(%)	RMSE	rRMSE	nRMSE(%)
<i>T</i>	13.78	0.73	4.29	8.14	0.45	2.45
<i>ONI</i>	1.73	0.09	0.54	4.18	0.23	1.26
<i>DIM</i>	0.52	0.03	0.16	0.57	0.03	0.17
Cessation over A				cessation over B		
<i>DIM</i>	0.76	0.08	0.87	0.80	0.07	0.94
Onset over A				Onset over B		
	MAE	rMAE	nMAE	MAE	rMAE	nMAE
<i>T</i>	13.74	0.73	7.30	2.20	0.40	4.27
<i>ONI</i>	0.72	0.04	2.33	0.70	0.13	0.22
<i>DIM</i>	0.14	0.01	0.12	0.04	0.01	0.05
Cessation over A				cessation over B		
<i>DIM</i>	0.33	0.03	0.31	0.36	0.03	0.39

Table 4: Forecast of the onset dates and the demise dates of the rainy seasons over the region A and the region B, with each, their error in days

	<i>region A</i>	<i>region B</i>
<i>Predictors</i>	Onset dates	
<i>Temperatures</i>	11/06/2017(±7)	11/23/2017(±3)
	11/06/2018(±7)	11/25/2018(±3)
<i>ONI</i>	11/22/2022(±5)	11/25/2022(±12)
	11/22/2023(±5)	10/17/2023(±12)
	11/23/2024(±5)	11/26/2024(±12)
<i>DIM</i>	22/11/2022(±5)	11/22/2022(±7)
	11/22/2023(±5)	11/22/2023(±7)
	11/23/2024(±5)	11/23/2024(±7)
	Demise dates	
<i>DIM</i>	03/27/2022(±4)	03/26/2022(±5)
	03/27/2023(±4)	03/26/2023(±5)
	04/14/2024(±4)	03/27/2024(±5)

9. **Figures**

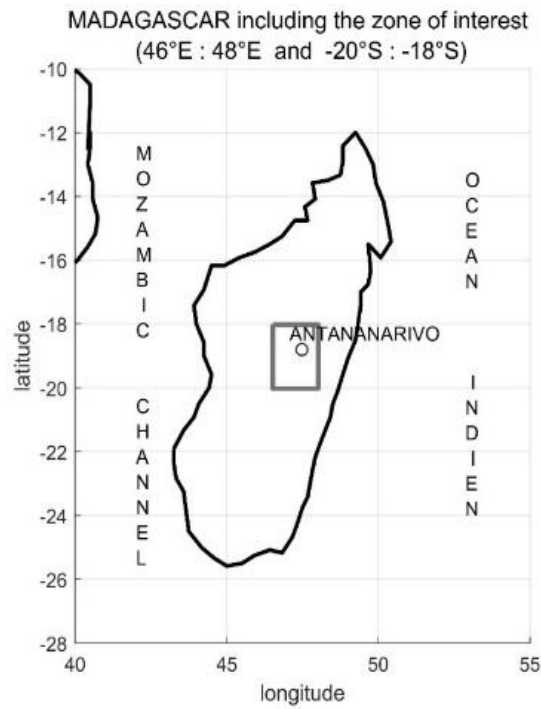


Figure 1: The zone of interest

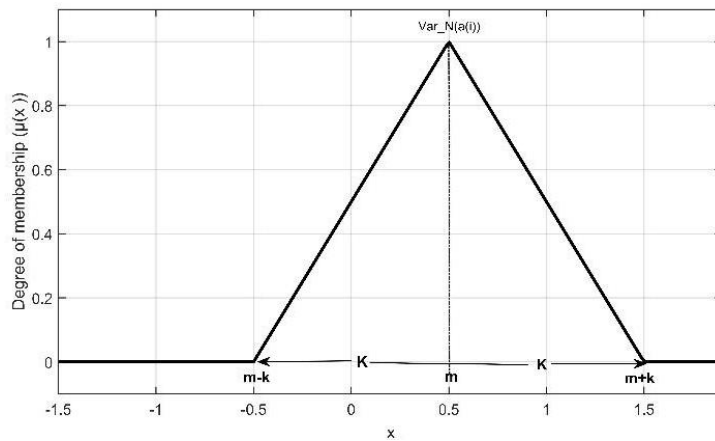


Figure 2: A representation of a triangular membership function

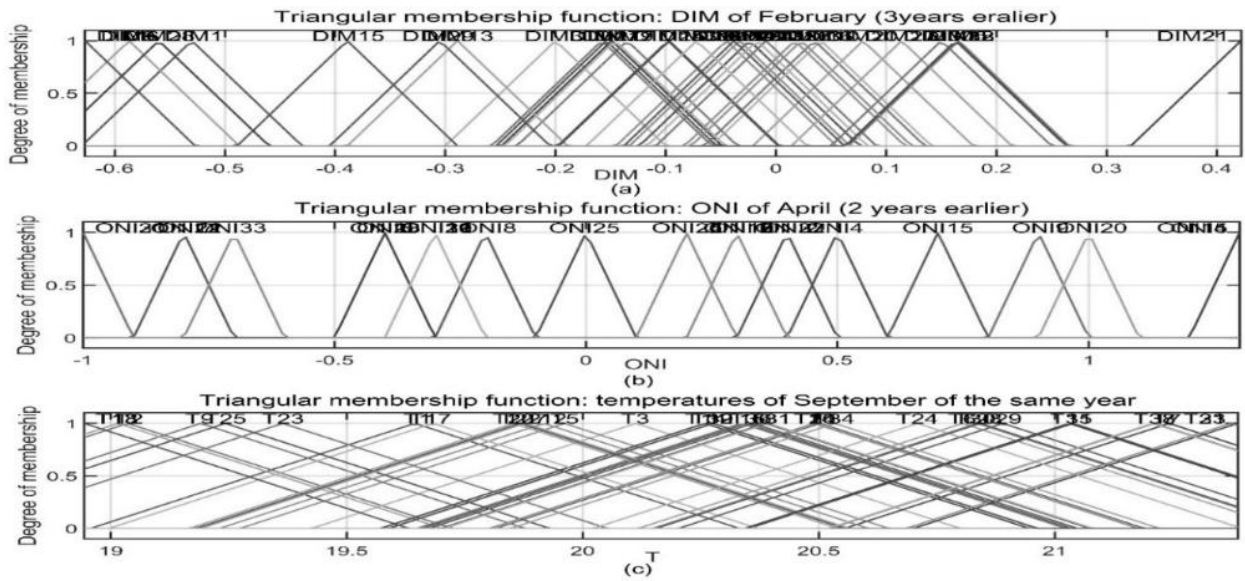


Figure 3: Examples of triangular membership functions related to: Dipole Index Mode (a) ;  
Oceanic Niño Index (b) and temperatures (c)

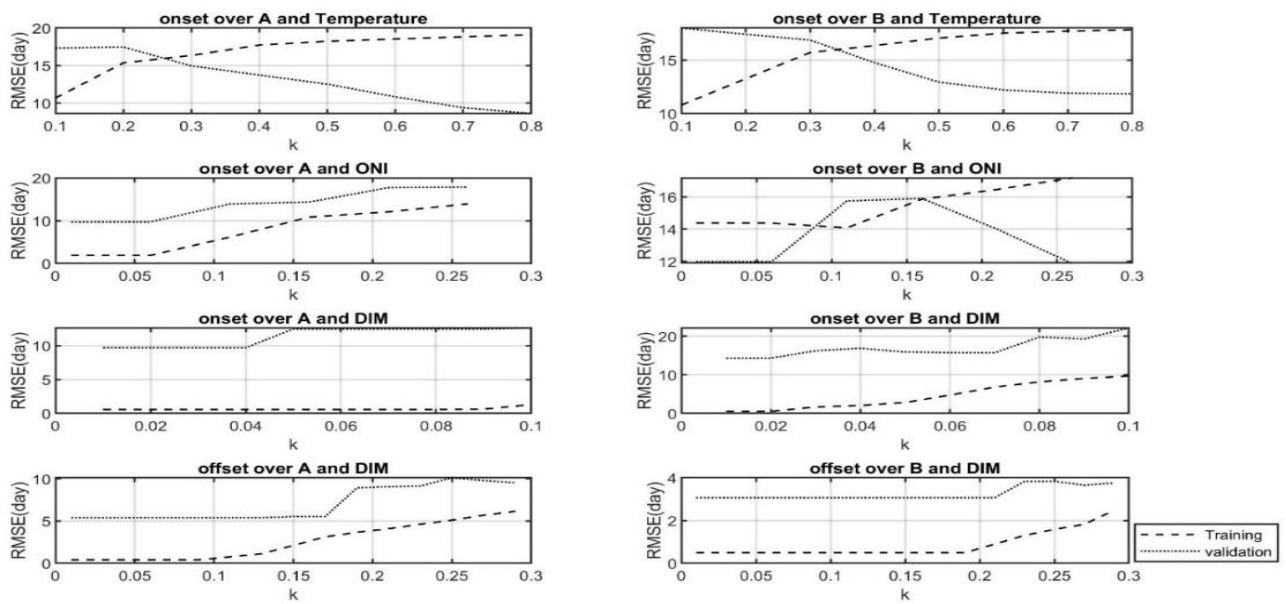


Figure 4: Different values of RMSE related to different values of 'k' corresponding to the training (---) and the validation (...) of the onset and cessation dates of the rainy seasons over A and B

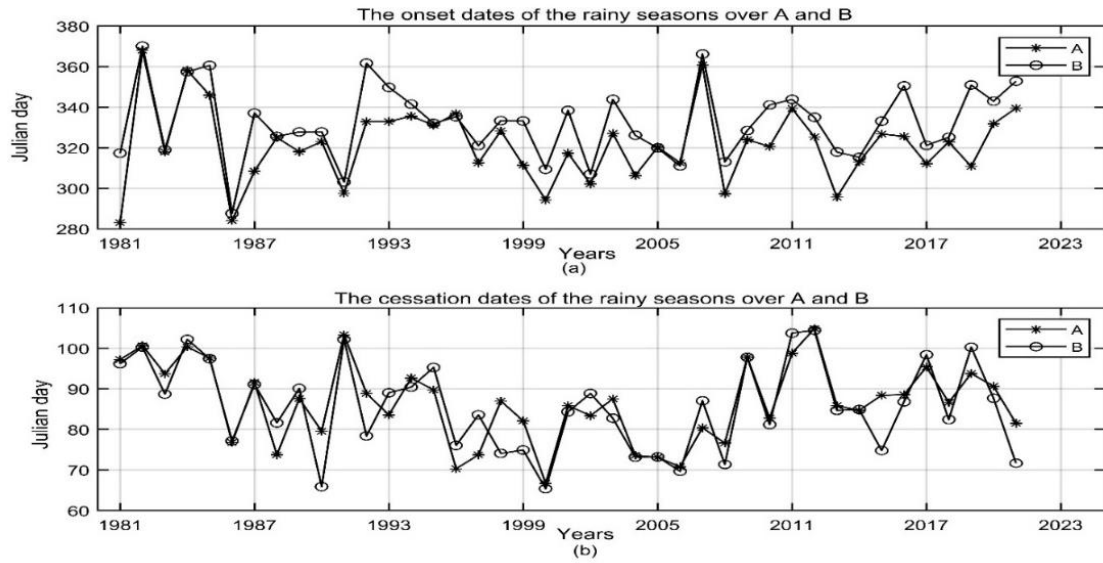


Figure 5: Evolution of the onset (a) and cessation (b) dates of the rainy seasons over both regions A and B from 1981 to 2021)

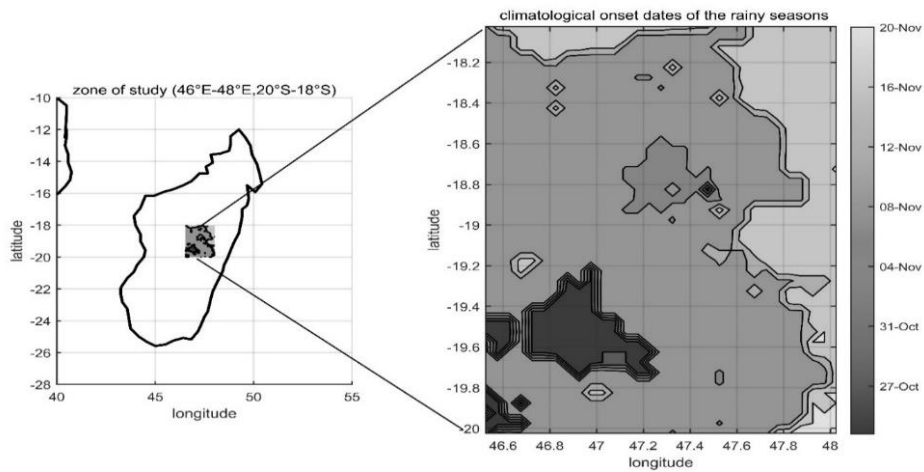


Figure 6: Spatial distribution of the climatological onset dates of the rainy seasons from 1981 to 2021 over the zone of interest

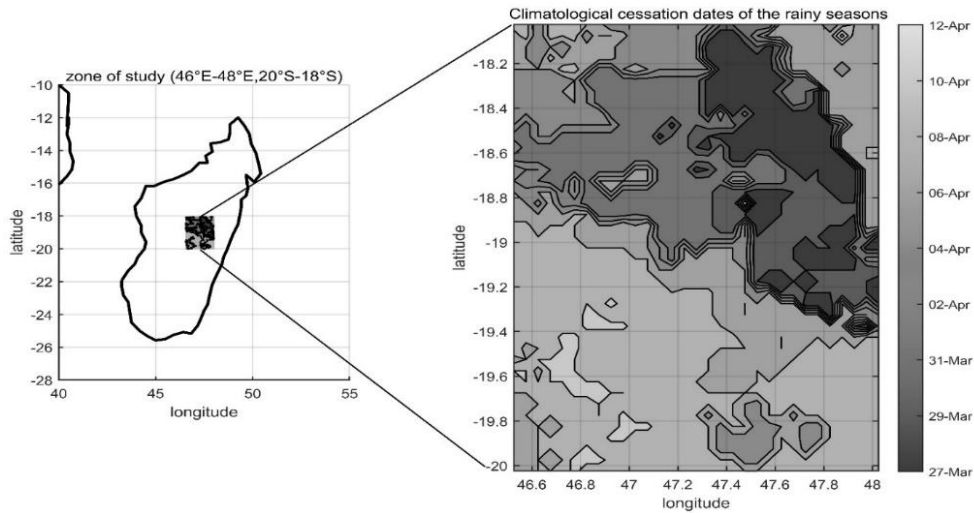


Figure 7: Spatial distribution of the climatological cessation dates of the rainy seasons from 1981 to 2021 over the zone of interest

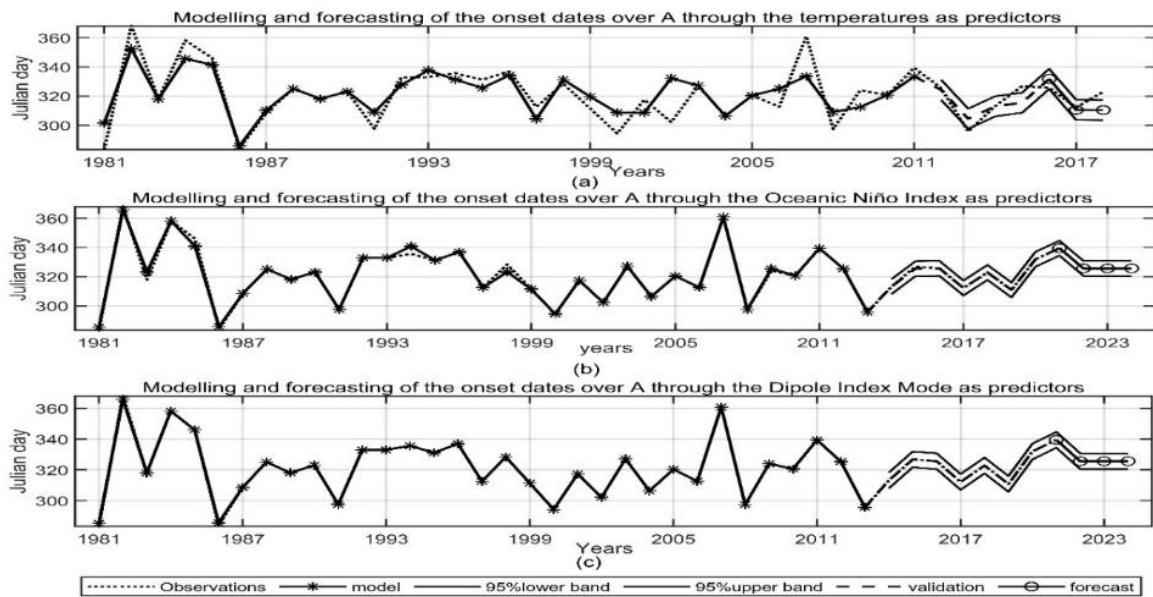


Figure 8: Modelling and forecasting of the onset dates of the rainy seasons with three predictors: the temperatures (a); the Oceanic Niño Index (b) and the Dipole Mode Index (c) over A

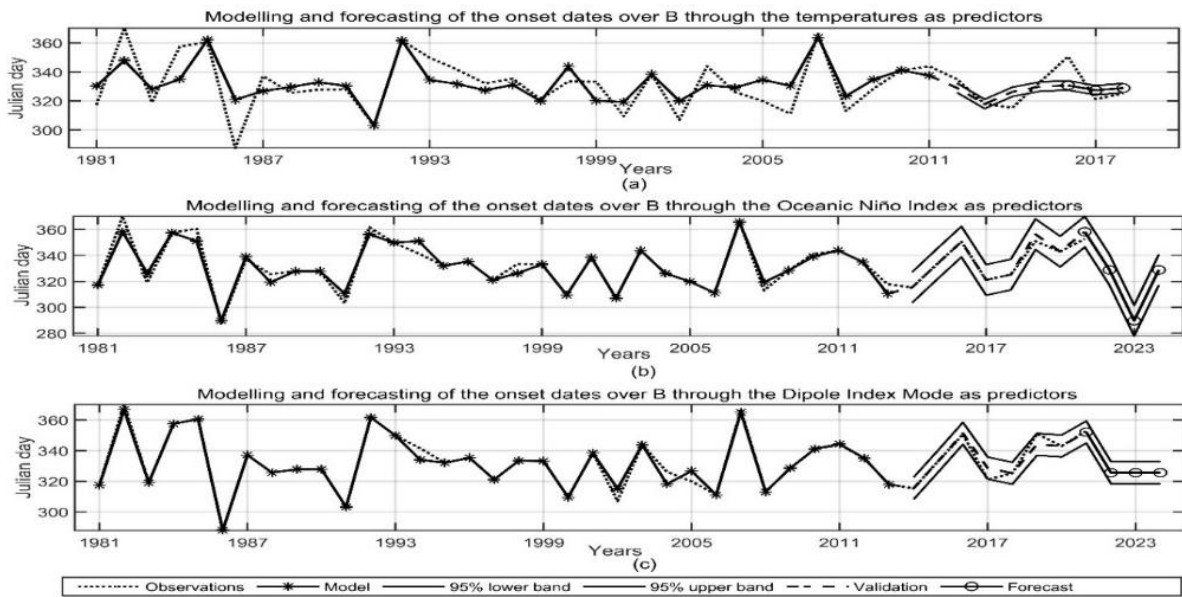


Figure 9: Modelling and forecasting of the onset dates of the rainy seasons with three predictors: the temperatures (a); the Oceanic Niño Index (b) and the Dipole Mode Index (c) over B.

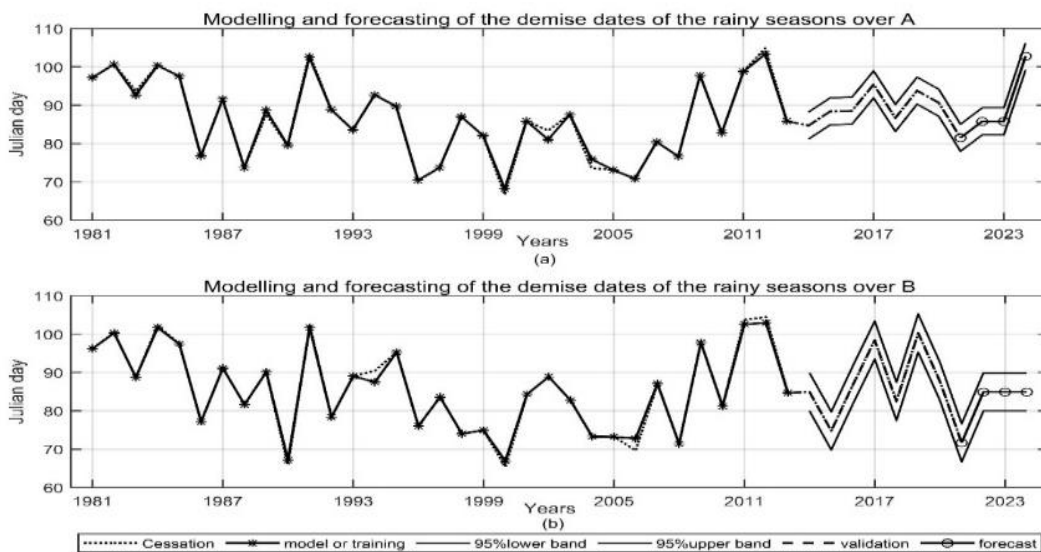


Figure 10: Modelling and forecasting of the cessation dates of the rainy seasons with the predictors: the Dipole Mode Index over A (a) and B (b)